

Theoretical and experimental investigations of new bis (amino triazole) schiff base ligand: Preparation of its $\text{UO}_2(\text{II})$, Er (III), and La (III) complexes, studying of their antibacterial, anticancer, and molecular docking

Reem G. Deghadi  | Ashraf A. Abbas  | Gehad G. Mohamed 

Chemistry Department, Faculty of Science, Cairo University, Giza, 12613, Egypt

Correspondence

Reem G. Deghadi, Chemistry Department, Faculty of Science, Cairo University, Giza 12613, Egypt.
Email: reemgd90@yahoo.com

$\text{UO}_2(\text{II})$, Er (III), and La (III) complexes were prepared from new bis (amino triazole) Schiff base ligand. The ligand was synthesized by condensation of 1,3-bis(4-amino-5-phenyl-1,2,4-triazol-3-ylsulfanyl)propane with benzaldehyde. The structure of the prepared compounds was confirmed by some spectroscopic tools such as $^1\text{H-NMR}$, UV-Vis, and IR, as well as molar conductance, mass spectrometry, elemental analysis, thermogravimetric analysis (TG), differential thermogravimetric (DTG), and differential thermal analysis (DTA) studies. The data revealed coordination of the complexes with tetradentate Schiff base. All complexes were octahedral. Computational studies for the prepared ligand by using DFT/B3LYP method were reported. The theoretical results described its bond lengths, angles, and dipole moment, and other parameters were calculated. The theoretical studies were supported the experimental data of the ligand and confirmed its successful preparation. Also, their antibacterial activities against four types of bacteria species (*Pseudomonas aeruginosa*, *Escherichia coli*, *Bacillus subtilis*, and *Staphylococcus aureus*) were investigated. The prepared complexes were biologically active compounds. The synthesized compounds were estimated for their anticancer activities against two cell lines (MCF-7 and HepG2). The lowest IC_{50} values were 17.6 and 23 μM for uranyl complex against MCF-7 and ligand against HepG2 cell lines, respectively, which make them very important materials as anticancer drugs in the future researches. Finally, molecular docking studies were checked up for all prepared compounds with different protein receptors (3HB5 and 2GYT) to confirm their anticancer activities data.

KEYWORDS

Er (III) complex, La (III) complex, MOE studies, triazole Schiff base, uranyl (II) complex

1 | INTRODUCTION

There has been various effort toward the improvement of novel chemical compounds which able to reverse or arrest the development of cancer.^[1] The transition metal

complexes derived from Schiff base ligands have applicable biological activities, so they considered as one of the most exhaustively studied topic in coordination chemistry. This may be due to their enhanced activities compared to non-Schiff base complexes.^[2,3]

Most prepared Schiff bases are easily accessible using simple synthetic procedures and with careful selection of a carbonyl compound and an amine precursor. The Schiff base ligands could potentially stabilize metals in different oxidation states and induce stability in heterogeneous and homogeneous catalysts.^[4] Schiff base metal complexes have various applications in different research areas, such as catalysis, molecular magnetism, and medical sciences.^[5,6] A large number of various Schiff base complexes have been used in several fields, such as materials science like optical switching, solar cell, third-order non-linear optics, Langmuir films, electrochemical sensing, and photo-initiated polymerization.^[7,8] Furthermore, they have important biological applications as antifungal, antibacterial, antiviral, anti-protozoal, anti-HIV, and anti-cancer agents.^[9–12]

The 1,2,4-triazole nucleus is the main structural unit of many medicines currently in market.^[13] Letrozole, fluconazole, ribavirin, anastrozole, and itraconazole are a few to name which are currently in use as medicines. 1,2,4-Triazole and its heterocyclic derivatives have great attention due to their synthetic and effective biological importance. The 1,2,4-triazole moieties had been incorporated into a different therapeutically interesting drug candidates, such as anti-migraine (rizatriptan), antiviral (ribavirin), antianxiety (alprazolam), and antifungal (fluconazole) compounds.^[14] 1,2,4-Triazoles and their derivatives have magnificent applications as antiviral, antifungal, antibacterial, antiasthmatic, pesticidal, hypnotic, breast cancer preventive, anticancer, antiinflammatory, anticonvulsant, CNS depressant, and antihypertensive.^[15] Furthermore, they may be used as mimics, isosteres, plant growth regulating, anticoagulant properties, and psychotropic, vasodilatory, 5-lipoxygenase, and cyclooxygenase inhibition.^[15] It has been reported that triazoles are less susceptible to metabolic degradation and have wider spectrum of activities and higher target specificity as compared to imidazoles.^[16] Moreover, the incorporation of azomethine Schiff base linkage into 1,2,4-triazole scaffold resulted in the formation of several therapeutically active compounds, which may significantly potentiate the antimicrobial activities.^[17]

So transition metal complexes of 1,2,4-triazole Schiff base have great importance due to their excellent coordination potential and wonderful pharmacological properties in antibacterial, antitumor, and antifungal activities. Letrozole, vorozole, and anastrozole are commercially 1,2,4-triazole drugs that can be used in treatment of breast cancer. Also, fluconazole that used as antifungal drugs and trazodone is known for its antidepressant properties.^[18]

During the development of actinide chemistry over the last six decades, it is obvious that uranyl ion with

the two axial coordination sites occupied by oxo groups can interact with different ligands in the equatorial plane to give four, five, or six coordination sites.^[19] The uranyl-salophen complex was previously prepared, which had pentagonal bipyramidal geometry structure. The two oxygen atoms of the $\text{UO}_2(\text{II})$ were in the apical positions, while the U atom was coordinated with the four donor atoms of the salophen ligand.^[20] This complex could be used as catalysts, sensors, or molecular recognition.^[21]

Lanthanides coordination compounds are the subject of intense research efforts owing to their unique structures and their potential applications in advanced materials such as Ln doped semiconductors, magnetic, catalytic, fluorescent, and nonlinear optical materials. The coordination chemistry of lanthanide (III) ions is very importance, due to incorporation of these compounds in basic and applied research in various scientific areas such as chemistry, material science, and life science. Nowadays, erbium atom enters in preparation of different and important metal complexes. Duo to its optical fluorescent properties, erbium-doped crystals can be used as optical amplification media and photographic filter.^[22] On the basis of the above facts, it was conducted in this research article to synthesize and characterize uranyl (II), erbium (III), and lanthanum (III) complexes with a new tetradentate triazole Schiff base. The ligand and its complexes were prepared, and their structure was established by using different spectroscopic tools. Also, we interested in comparing the theoretical data by DFT/B3LYP method with the experimental results for confirming the structure of the ligand. Their antibacterial activities against four different species were screened, and their anticancer activities were investigated against two cell lines MCF-7 and HepG2. The mode of binding between different protein receptors and the reported compounds was studied using molecular docking.

2 | EXPERIMENTAL

2.1 | Materials and reagents

All chemicals used were very pure and of the analytical reagent grade (AR). The chemicals used included 4-amino-5-phenyl-1,2,4-triazole-3-(2H)-thione, 1,3-dibromopropane, benzaldehyde, $\text{UO}_2(\text{NO}_3)_2$, $\text{ErCl}_3 \cdot 6\text{H}_2\text{O}$ and $\text{LaCl}_3 \cdot 7\text{H}_2\text{O}$ were supplied from Sigma-Aldrich. Organic solvents that used were ethyl alcohol (95%), *N,N*-dimethylformamide (DMF), KOH, and glacial acetic acid. Deionized water was usually used in all preparations.

2.2 | Solutions

Stock solutions of the Schiff base ligand and its metal complexes of 1×10^{-3} M were prepared by dissolving an accurately weighed amount in DMF. Then, the conductivity measured for 1×10^{-3} M solution of the metal complexes. Dilute solutions of the Schiff base ligand and its metal complexes (1×10^{-4} M) were prepared by accurate dilution from the previous prepared stock solutions for measuring their UV-Vis spectra.

2.3 | Instrumentation

Microanalyses of carbon, hydrogen, and nitrogen were carried out at the Microanalytical Center, Cairo University, Egypt, using a CHNS-932 (LECO) Vario elemental analyzer. Analyses of the metals were conducted by dissolving the solid complexes in concentrated HNO_3 and dissolving the residue in deionized water. The metal content was carried out using inductively coupled plasma atomic absorption spectrometry (ICP-AES), Egyptian Petroleum Research Institute. Fourier transform infrared (FT-IR) spectra were recorded with a PerkinElmer 1650 spectrometer ($400\text{--}4,000\text{ cm}^{-1}$) as KBr pellets. $^1\text{H-NMR}$ spectra, as solutions in DMSO-d_6 , were recorded with a 300 MHz Varian-Oxford Mercury at room temperature using TMS as an internal standard. Mass spectra were recorded using the electron ionization technique at 70 eV with an MS-5988 GS-MS Hewlett-Packard instrument at the Microanalytical Center, National Center for Research, Egypt. UV-Visible spectra were obtained with a Shimadzu UVmini-1240 spectrophotometer. Molar conductivities of 1×10^{-3} M solutions of the solid complexes were measured using a Jenway 4010 conductivity meter. Thermogravimetric (TG), differential thermal analysis (DTA), and differential thermogravimetric (DTG) analyses of the solid compounds were carried out from room temperature to $1,000^\circ\text{C}$ using a Shimadzu TG-50H thermal analyzer. Antibacterial measurements were carried out at the Microanalytical Center, Cairo University, Egypt. Anti-cancer activity experiments were performed at the National Cancer Institute, Cancer Biology Department, Pharmacology Department, Cairo University. The

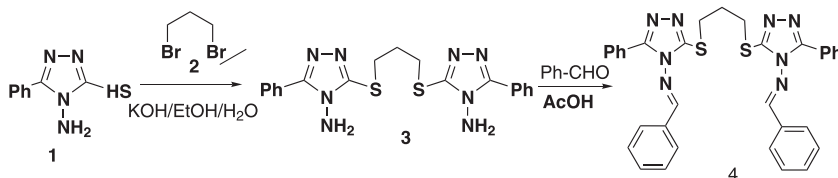
optical density (OD) of each well was measured spectrophotometrically at 564 nm with an ELIZA microplate reader (Meter tech. R960, USA). The powder X-ray diffraction (PXRD) was recorded by Bruker D8 Discover (Bruker AXS Inc., 35 KV, 30 mA) X-ray diffractometer in Egypt Nanotechnology Center (EGNC), with a step size of 0.02 and speed scan 0.016 using $\text{Cu K}\alpha$ radiation ($\lambda = 1.5406\text{ \AA}$) for 2 h with 2θ ranging between 5 and 70.

2.4 | Synthesis of bis (amino triazole) Schiff base ligand (L)

4-amino-5-phenyl-1,2,4-triazole-3(2H)-thione (**1**) was reacted with 1,3-dibromopropane (**2**) in ethanol-water (1:1) mixture containing KOH to give the corresponding 1,3-bis(4-amino-5-phenyl-1,2,4-triazol-3-ylsulfanyl)propane (**3**). Condensation of the latter compound with benzaldehyde in glacial acetic acid afforded the corresponding Schiff base 1,3-bis(4-benzylideneamino-5-phenyl-1,2,4-triazol-3-ylsulfanyl)propane (**L**) (**4**) in 65% yield as shown in Scheme 1.

To a solution of **1** (50 mmol) in ethanol-water mixture (50 ml, 50%) containing KOH (50 mmol) was added 1,3-dibromopropane (**2**) (25 mmol). The reaction mixture was heated under reflux for 1 h. The solvent was then removed in vacuo, and the remaining solid was collected and crystallized from DMF to give colorless crystals of compounds (**3**) as previously prepared.^[23]

To a solution of each of **3** (20 mmol) in glacial acetic acid (15 ml) was added benzaldehyde (40 mmol). The reaction mixture was heated under reflux for 2 h. The solvent was then removed in vacuo, and the remaining solid was collected and crystallized from ethanol as colorless crystals (compound **4**) (65%, mp. 168°C ; %). FT-IR (ν , cm^{-1}): azomethine ($\text{CH}=\text{N}$) 1,603sh, triazole ($\text{C}=\text{N}$) 1571sh, ($\text{C}-\text{S}$) 767sh. $^1\text{H-NMR}$ (DMSO) δ 2.35 (quintet, 2H, $J = 6.6\text{ Hz}$, SCH_2CH_2), 3.44 (t , 4H, $J = 6.6\text{ Hz}$, SCH_2), 7.42–7.91 (m, 20H, ArH's), 8.50 (s, 2H, $\text{CH}=\text{N}$) ppm. Anal. for $\text{C}_{33}\text{H}_{28}\text{N}_8\text{S}_2$ (600.76 g/mol) Calc.: C, 65.98; H, 4.70; N, 18.65. Found: C, 65.97; H, 4.82; N, 18.58%. UV-Vis (λ_{max} , nm): 251 ($\pi-\pi^*$ of phenyl groups) and 342 ($n-\pi^*$ of $\text{CH}=\text{N}$ azomethine group).



SCHEME 1 Synthesis of Schiff base ligand 4

2.5 | Synthesis of metal complexes

UO₂(II), Er (III), or La (III) complexes were prepared by a reaction of 1:1 molar mixture of hot ethanolic solution (60°C) of UO₂(NO₃)₂ (0.263 g, 6.67 × 10⁻⁴ mol), ErCl₃·6H₂O (0.255, 6.67 × 10⁻⁴ mol) or LaCl₃·7H₂O (0.248 g, 6.67 × 10⁻⁴ mol) and DMF solution of Schiff base ligand (L) (0.4 g, 6.67 × 10⁻⁴ mol). The resulting compounds were stirred under refluxing for 1 h, whereupon the complexes precipitated. They were collected by filtration and purified by washing several times with diethyl ether. The solid complexes then dried in desiccator over anhydrous calcium chloride.

2.5.1 | [UO₂(I)].2NO₃

Yield 75%; m.p. 156°C; yellow precipitate. Anal. Calc. for C₃₃H₂₈UN₁₀O₈S₂ (%): C, 39.94; H, 2.82; N, 14.09; U, 23.94. Found (%): C, 39.01; H, 2.19; N, 14.82; U, 23.12. Λ_m (Ω⁻¹ mol⁻¹ cm²) = 134; FT-IR (ν, cm⁻¹): azomethine (CH=N) 1646sh, triazole (C=N) 1,571 s, asy (O=U=O) 921, sym (O=U=O) 826, (C—S) 772 m, (M—N) 499 s, (M—S) 454w. UV-Vis (λ_{max}, nm): 250 (π-π* of phenyl groups) and 331 (n-π* of C=N azomethine group). ¹H-NMR (DMSO) δ 2.49 (quintet, 2H, SCH₂CH₂), 3.32 (t, 4H, SCH₂), 7.48–7.90 (m, 20H, ArH's) and 8.87 (s, 2H, CH=N) ppm.

2.5.2 | [Er(L)(H₂O)cl]Cl₂.3H₂O

Yield 80%; m.p. 237°C; pink precipitate. Anal. Calc. for C₃₃H₃₆Cl₃ErN₈O₄S₂ (%): C, 41.87; H, 3.81; N, 11.84; Er, 17.66. Found (%): C, 41.22; H, 3.75; N, 11.62; Er, 17.01. Λ_m (Ω⁻¹ mol⁻¹ cm²) = 130; FT-IR (ν, cm⁻¹): azomethine (CH=N) 1,634 m, triazole (C=N) 1,572 s, H₂O stretching of coordinated water 924w and 880w, (C—S) 758 s, (M—O) 577 s, (M—N) 501 s, (M—S) 454w. UV-Vis (λ_{max}, nm): 250 (π-π* of phenyl groups) and 334 (n-π* of C=N azomethine group). ¹H-NMR (DMSO) δ 2.50 (quintet, 2H, SCH₂CH₂), 3.34 (t, 4H, SCH₂), 7.48–7.90 (m, 20H, ArH's) and 8.86 (s, 2H, CH=N) ppm.

2.5.3 | [La(L)(H₂O)cl]Cl₂.4H₂O

Yield 75%; m.p. 180°C; ivory precipitate. Anal. Calc. for C₃₃H₃₈Cl₃LaN₈O₅S₂ (%): C, 42.33; H, 4.06; N, 11.97; La, 14.86. Found (%): C, 41.98; H, 3.75; N, 11.29; La, 14.01. Λ_m (Ω⁻¹ mol⁻¹ cm²) = 119; FT-IR (ν, cm⁻¹): azomethine (CH=N) 1,656sh, triazole (C=N) 1,572w, H₂O stretching of coordinated water 924w and 880w, (C—S) 761 s,

(M—O) 578w, (M—N) 506w, (M—S) 417w. UV-Vis (λ_{max}, nm): 251 (π-π* of phenyl groups) and 338 (n-π* of C=N azomethine group). ¹H-NMR (DMSO) δ 2.50 (quintet, 2H, SCH₂CH₂), 3.25 (t, 4H, SCH₂), 7.46–7.94 (m, 20H, ArH's) and 8.86 (s, 2H, CH=N) ppm.

2.6 | Spectrophotometric studies

The absorption spectra were recorded for 1 × 10⁻⁴ M solutions of the free Schiff base ligand (L) and its metal complexes. The spectra were scanned within the wavelength range from 200 to 700 nm.

2.7 | Antibacterial activity

The in vitro antibacterial activity tests were performed through the disc diffusion method.^[24] The bacterial organisms that have been used were *Pseudomonas aeruginosa*, *Escherichia coli*, *Bacillus subtilis*, and *Staphylococcus aureus*. Stock solution (0.001 mol) was prepared by dissolving the compounds in DMSO. The nutrient agar medium for antibacterial was (0.5% peptone, 0.1% beef extract, 0.2% yeast extract, 0.5% NaCl, and 1.5% agar-agar) was prepared, cooled to 47°C and then seeded with tested microorganisms. After solidification 5 mm diameter holes were punched by a sterile corkborer. The investigated compounds, that is, Schiff base ligand (L) and its metal complexes, were introduced in Petri-dishes (only 0.1 m) after dissolving in DMSO at 1.0 × 10⁻³ M. These culture plates were then incubated at 37°C for 20 h for bacteria. By measuring the diameter of inhibition zone (in mm), the activity could be determined. The plates were kept for incubation at 37°C for 24 h, and then, the plates were examined for the formation of zone of inhibition. The diameter of the inhibition zone was measured in millimeters. Antimicrobial activities were performed in triplicate and the average was taken as the final reading.^[25]

2.8 | Anticancer activity

Potential cytotoxicity of all prepared compounds was tested using the method of Skehan and Storeng.^[26] Cells were plated in 96-multiwell plate (104 cells/well) for 24 h before treatment with the compounds to allow attachment of cell to the wall of the plate. Different concentrations of the compounds under investigation (5, 12.5, 25, 50, and 100 μM) were added to the cell monolayer, and triplicate wells were prepared for each individual

dose. The monolayer cells were incubated with the compounds for 48 h at 37°C and in 5% CO₂ atmosphere. After 48 h, the cells were fixed; then, they were washed and finally stained with SRB stain. To remove excess stain, they were washed with acetic acid, and attached stain was recovered with tris-EDTA buffer. The optical density (O.D.) of each well was measured spectrophotometrically at 564 nm with an ELIZA microplate reader, and the mean background absorbance was automatically subtracted, and mean values of each drug concentration were calculated. The relation between drug concentration and surviving fraction is plotted to get the survival curve of breast tumor cell line for each compound.

2.8.1 | Calculation

The % of cell survival was calculated according to the following relation:

Survival fraction = O.D. (treated cells) / O.D. (control cells). The IC₅₀ values (the concentrations of the Schiff base ligand (L) or complexes required to produce 50% inhibition of cell growth). This experiment was repeated three times.

2.9 | Molecular docking

Molecular docking studies were elaborated using MOE 2008 software, and it is a rigid molecular docking software. These studies are very important for predicting the possible binding modes of the most active compounds against the receptors of breast cancer mutant oxidoreductase (PDB ID: 3HB5) and crystal structure of the liver cancer (PDB ID: 2GYT).^[27] Docking is an interactive molecular graphics program which can be used to calculate and display feasible docking modes of a receptor, ligand, and complex molecules. It necessitates the ligand, the receptor as input in PDB format. The water molecules, co-crystallized ligands, and other unsupported elements (e.g., Na, K, and Hg) were removed, but the amino acid chain was kept.^[28] The structure of ligand in PDB file format was created by Gaussian09 software. The crystal structures of the three receptors were downloaded from the protein data bank (<http://www.rcsb.org./pdb>).

2.10 | Computational methodology

Molecular modeling theoretical calculations and DFT studies for the prepared triazole Schiff base ligand (L) were carried out on the Gaussian03 package,^[29] by

using density functional theory (DFT). The molecular geometry for the prepared ligand was fully optimized by using density functional theory (DFT) which based on the B3LYP method along with the LANL2DZ basis set. The structure of the ligand (L) was first optimized by using Chemcraft version 1.6 package^[30] and GaussView version 5.0.9.^[31]

3 | RESULTS AND DISCUSSION

3.1 | Experimental characterization of the ligand (L) and its metal complexes

The structure of the ligand, UO₂(II), Er (III), and La (III) complexes were confirmed by using different spectroscopic and physicochemical techniques. These analyses are elemental analysis (C, H, N, and M), molar conductance, IR, ¹H-NMR, UV-Vis, mass spectrometry, XRD, and thermal analyses.

3.1.1 | Elemental analysis

The results of elemental analysis together with some physical properties such as color and melting point were reported previously in experimental part. The data of the new prepared Schiff base ligand (L) (compound 4) was Anal. calc.: C, 65.98; H, 4.70; N, 18.65. Found: C, 65.97; H, 4.82; N, 18.58%. That proved the proposed molecular formulas C₃₃H₂₈N₈S₂ of the ligand. Also, the analytical data of the metal complexes indicated that the complexes have 1:1 (metal: ligand) stoichiometry ratio. The prepared compounds were colorless, yellow, pink, and ivory colored crystals for ligand, uranyl (II), erbium (II), and lanthanum (III) complexes, respectively. They are non-hygroscopic, stable at room temperature, and soluble in DMF and DMSO solvents.

3.1.2 | Molar conductivity measurements

The UO₂(II), Er (III), and La (III) complexes were dissolved in DMF solvent. Their molar conductivities of the 1 × 10⁻³ mol L⁻¹ solutions at room temperature were measured. The conductivity measurements are tested the degree of ionization of the prepared complexes.^[32] The higher value of conductivity than 50 Ω⁻¹ mol⁻¹ cm² corresponds to the presence of counter ions outside the coordination sphere and vice versa. The results showed values of 134, 130, and 119 Ω⁻¹ mol⁻¹ cm² for [UO₂(L)]—2NO₃, [Er(L)(H₂O)Cl]Cl₂—3H₂O, and [La(L)(H₂O)Cl]Cl₂—4H₂O complexes, respectively. It is

considered as 1:2 electrolytes where two chloride ions are present outside the coordination sphere in Er (III) and La (III) complexes. And two nitrate groups were presented outside the coordination sphere in $\text{UO}_2(\text{II})$ complex.^[33]

3.1.3 | IR spectra

The structure of triazole Schiff base is confirmed by the appearance of new strong azomethine ν ($\text{CH}=\text{N}$) band at $1,603\text{ cm}^{-1}$ in its spectrum.^[34] Also, the spectrum of the ligand showed band at $1,571\text{ cm}^{-1}$ corresponded to $\nu(\text{C}=\text{N})$ of triazole moiety and 767 cm^{-1} of $\text{C}-\text{S}$ bond.^[35,36]

In IR spectrum of uranyl (II) complex, it reported that azomethine ν ($\text{CH}=\text{N}$) band appeared at $1,646\text{ cm}^{-1}$. This band shifted by about 43 cm^{-1} , indicating the participation of this group in coordination. The triazole group still appeared at the same value as at the free ligand. Furthermore, there are shifting in the band of $\nu(\text{C}-\text{S})$ which appeared in the complex at 772 cm^{-1} confirming the second participation of the ligand with the metal ion. The spectrum of uranyl complex showed two bands at 921 and 826 cm^{-1} assigned to $\nu_{\text{asy}}(\text{O}=\text{U}=\text{O})$ and $\nu_{\text{sy}}(\text{O}=\text{U}=\text{O})$, respectively.^[37] These results exhibited that the UO_2 moiety is virtually linear.^[38] New band observed in the complex at 499 cm^{-1} which related to $\nu(\text{U}-\text{N})$, while the band appeared at 454 cm^{-1} was corresponded to $\nu(\text{U}-\text{S})$.^[18,34] The spectrum also exhibited band at $1,385\text{ cm}^{-1}$ corresponded to an uncoordinated nitrate group.^[36] The IR spectrum of $\text{UO}_2(\text{II})$ complex exhibited two non-ligand bands at $1,448$ and $1,256\text{ cm}^{-1}$ which support the monodentate nature of NO_3 group.^[39,40]

The same observation in IR spectrum of Er (III) complex, which the azomethine group was shifted by about 31 cm^{-1} , and $\text{C}-\text{S}$ band was appeared at 758 cm^{-1} . These results confirmed the involvement of these four heteroatoms in coordination. The triazole band also appeared at the same position as in the free ligand. New bands were observed at 577 and 501 cm^{-1} related to (Er—O) and (Er—N) vibrations.^[41] The band appeared at 454 cm^{-1} was corresponded to ν (Er—S). The ν (Er—OH₂) bands were appeared at 924 and 880 cm^{-1} that indicated the participation of water molecule in the coordination.^[42]

Furthermore, in IR spectrum of La (III) complex, the azomethine group was shifted by about 53 cm^{-1} , and $\text{C}-\text{S}$ band was appeared at 761 cm^{-1} . These data confirmed the involvement of these sites also in coordination. The triazole band appeared at the same position as in the free ligand. New bands were observed at 576 and 506 cm^{-1} related to (La—O) and (La—N) vibrations.^[41] The band appeared at 417 cm^{-1} was corresponded to ν

(La—S). The ν (La—OH₂) bands were appeared at 924 and 880 cm^{-1} that indicated the participation of water molecule in the coordination.^[42]

The four IR spectra of the prepared compounds were shown in Figure 1. The results of IR showed that the ligand behaved as a neutral tetradentate ligand that coordinated to metal ions via four sites of donation (N, N, S, and S).

3.1.4 | ¹H-NMR spectra

The ¹H-NMR spectra of the Schiff base ligand (L), $[\text{UO}_2(\text{L})]-2\text{NO}_3$, $[\text{Er}(\text{L})(\text{H}_2\text{O})\text{Cl}]\text{Cl}_2-3\text{H}_2\text{O}$, and $[\text{La}(\text{L})(\text{H}_2\text{O})\text{Cl}]\text{Cl}_2-4\text{H}_2\text{O}$ complexes were studied. The spectrum of the ligand showed signals at 2.35 (quintet, 2H, $J = 6.6\text{ Hz}$, SCH_2CH_2), 3.44 (t, 4H, $J = 6.6\text{ Hz}$, SCH_2), 7.42–7.91 (m, 20H, ArH's), and 8.50 (s, 2H, $\text{CH}=\text{N}$) ppm.^[43–45]

The spectrum of $[\text{UO}_2(\text{L})]-2\text{NO}_3$ complex showed signals at 2.49 (quintet, 2H, SCH_2CH_2), 3.32 (t, 4H, SCH_2), 7.48–7.90 (m, 20H, ArH's), and 8.87 (s, 2H, $\text{CH}=\text{N}$) ppm. While, spectrum of $[\text{Er}(\text{L})(\text{H}_2\text{O})\text{Cl}]\text{Cl}_2-3\text{H}_2\text{O}$ complex indicated signals at 2.50 (quintet, 2H, SCH_2CH_2), 3.34 (t, 4H, SCH_2), 7.48–7.90 (m, 20H, ArH's), and 8.86 (s, 2H, $\text{CH}=\text{N}$) ppm. Also, spectrum of $[\text{La}(\text{L})(\text{H}_2\text{O})\text{Cl}]\text{Cl}_2-4\text{H}_2\text{O}$ complex indicated signals at 2.50 (quintet, 2H, SCH_2CH_2), 3.25 (t, 4H, SCH_2), 7.46–7.94 (m, 20H, ArH's), and 8.86 (s, 2H, $\text{CH}=\text{N}$) ppm. The signal corresponding to azomethine group was shifted from the free ligand by about 0.36, or 0.37 ppm, suggests the coordination through azomethine nitrogen of the ligand to erbium, lanthanum, or uranyl atoms. Also, there are shifting in signals of SCH_2CH_2 to higher values by about 0.14 in uranyl complex or 0.15 ppm in erbium and lanthanum complexes, and signals of SCH_2 to lower values by about -0.12 , -0.10 , and -0.19 ppm for $\text{UO}_2(\text{II})$, Er (III), and La (III) complexes, respectively. All spectra of the prepared compounds were reported in Figure 2. The ¹H-NMR results indicated the successful preparation of the Schiff base and its metal complexes.

3.1.5 | Mass spectra

The mass spectra of the ligand and its complexes were recorded and investigated at 70 eV of electron energy. It is recognized that the molecular ion peaks of the four prepared compounds are in good agreement with their suggested empirical formula as shown from elemental analyses. The ion peaks were 994.30, 945.40, 939.0, and 600.20 m/z which were compatible with their molecular weight of 994, 945.76, 935.5, and 600 g/mol for $\text{UO}_2(\text{II})$,

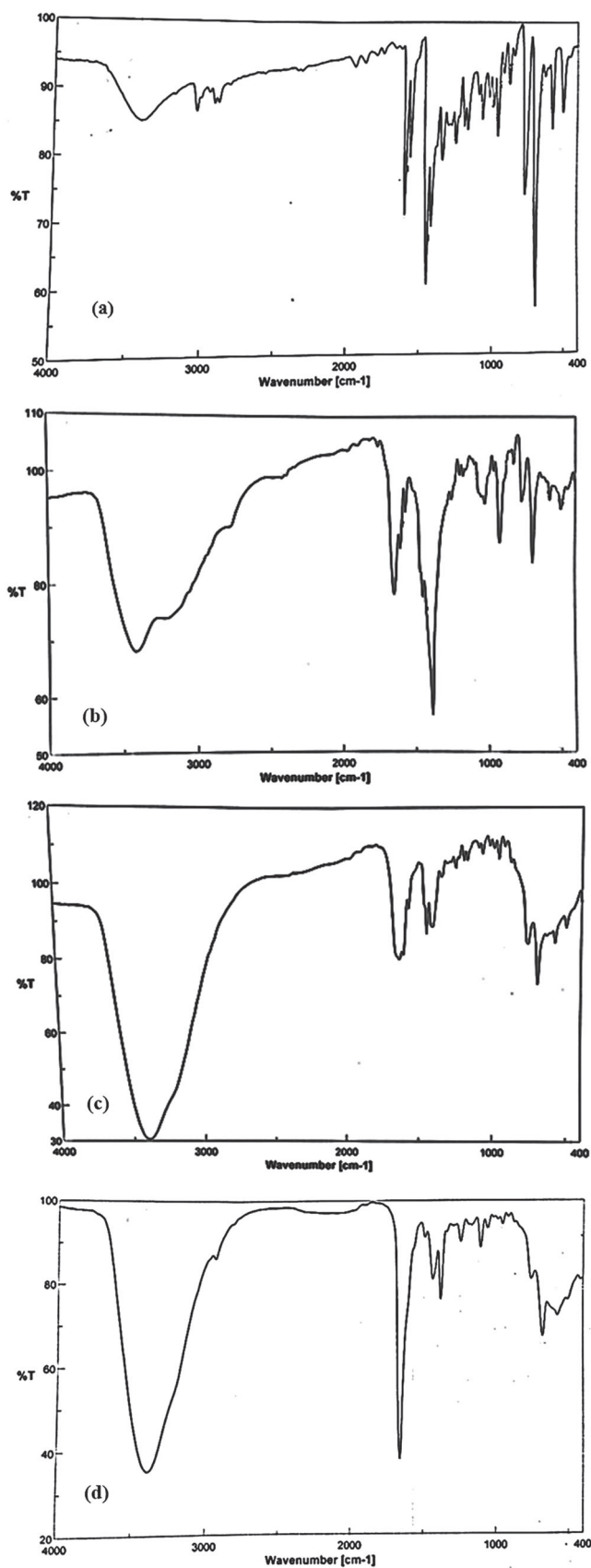


FIGURE 1 The IR spectra of (a) Schiff base ligand, (b) [Er(L)(H₂O)Cl]Cl₂·3H₂O, (c) [UO₂(L)]·2NO₃, and (d) [La(L)(H₂O)Cl]Cl₂·4H₂O

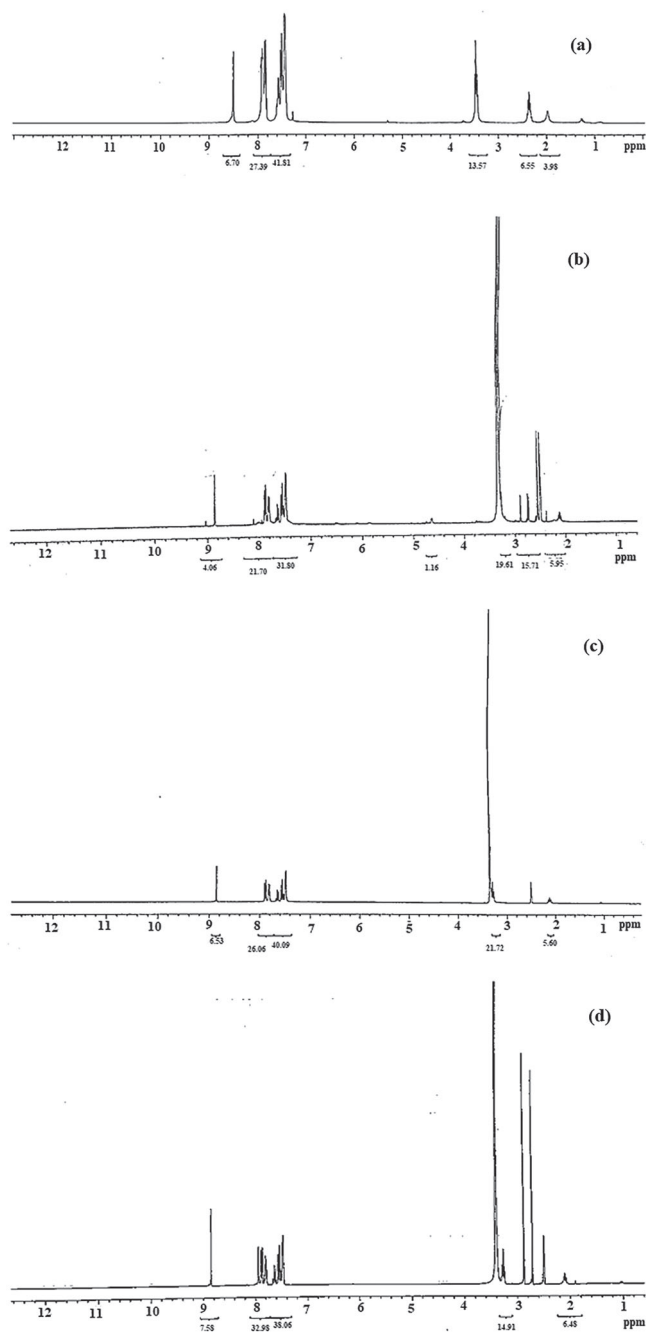


FIGURE 2 ¹H-NMR spectra of (a) Schiff base ligand, (b) [UO₂(L)]·2NO₃, (c) [Er(L)(H₂O)Cl]Cl₂·3H₂O, and (d) [La(L)(H₂O)Cl]Cl₂·4H₂O

Er (III), and La (III) complexes and Schiff base ligand (L), respectively. Then, the spectra were recorded in Figure S1.

3.1.6 | UV-visible spectra

The synthesis of UO₂(II)/Er (III)/La (III)-Schiff base complexes was also confirmed by using UV/Vis spectra.

Electronic spectra of the prepared Schiff base ligand (L) and its metal complexes were recorded in DMF solution, at wavelength range 200–700 nm with concentration 1×10^{-4} M. The spectrum of the ligand showed two absorption bands at 342 and 251 nm. The first band corresponded to $n-\pi^*$ transition of (CH=N) azomethine group in the free ligand.^[46] At which the second band related to $\pi-\pi^*$ transition of phenyl groups.^[47] The 342 value was shifted to 334 nm in Er (III) complex, while shifted in $\text{UO}_2(\text{II})$ complex to 331 nm and to 338 nm in La (III)-complex. This shifting confirmed the participation of the azomethine group in combination and coordination. The second band at 251 nm in the ligand appeared at the same region in the three complexes.

3.1.7 | X-ray diffraction

X-ray diffraction (XRD) was performed to obtain further evidence about the structure of the metal complexes.^[48] Also, it performed the average grain size, crystallinity, and other structural parameter. The diffractograms obtained for the Schiff base and its metal complexes were given in Figure 3. The XRD patterns of the compounds under investigation showed good intense peaks indicating high crystallinity of the prepared compounds. Except $[\text{La}(\text{L})(\text{H}_2\text{O})\text{Cl}]\text{Cl}_2 \cdot 4\text{H}_2\text{O}$ complex which had semi-crystalline behavior.

It can be clearly seen that the pattern of the Schiff base changed from its metal complexes, which may be approved to the formation of a well-defined distorted crystalline metal complexes structure.

3.1.8 | Thermal analysis of Schiff base ligand, $\text{UO}_2(\text{II})$, Er (III), and La (III) complexes

The thermal stability of the synthesized ligand (L) and its metal complexes was investigated by using thermogravimetric analysis (TG), differential thermogravimetric analysis (DTG), and differential thermal analysis (DTA) within the temperature range of 25–900°C. The results comprising temperature ranges, stages of decomposition, decomposition product lost, and the calculated mass loss percentages were listed in Table 1. And all TGA/DTG/DTA spectra were represented in Figure S2.

The thermal decomposition of the Schiff base ligand involved one decomposition step. It was started at 170°C and finished at 530°C, which involved the removal of $\text{C}_{33}\text{H}_{28}\text{N}_8\text{S}_2$ molecule (found 99.40% and calc. = 100%). The maximum temperature peak was at 262°C. No

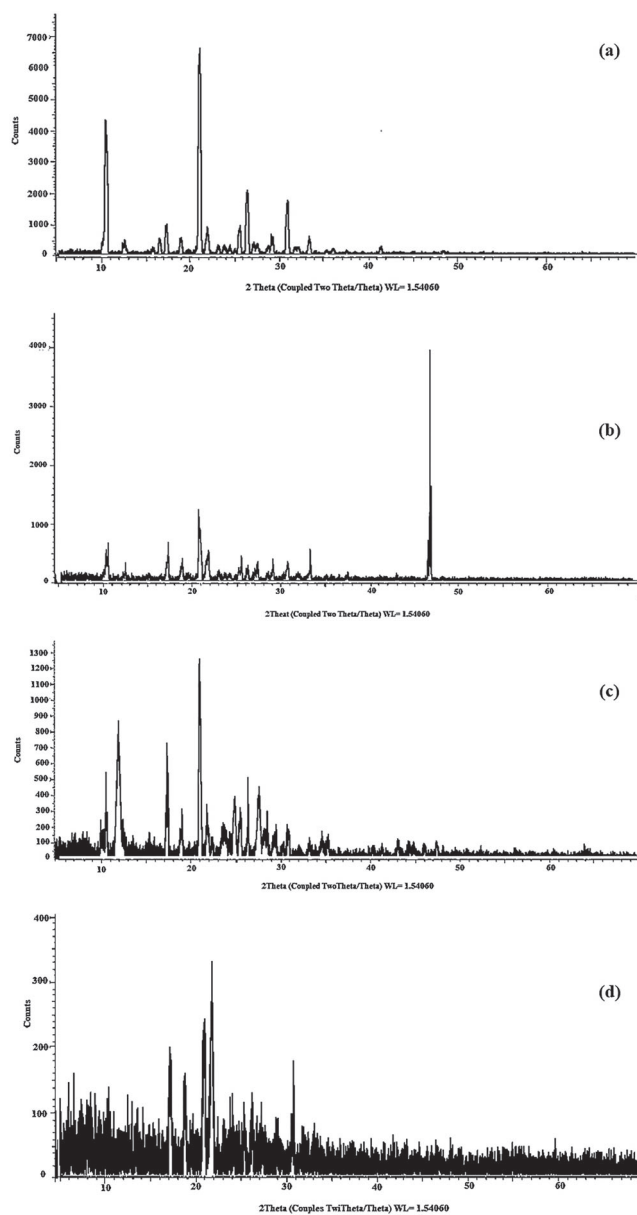


FIGURE 3 XRD patterns of (a) Schiff base ligand, (b) $[\text{UO}_2(\text{L})] \cdot 2\text{NO}_3$, (c) $[\text{Er}(\text{L})(\text{H}_2\text{O})\text{Cl}]\text{Cl}_2 \cdot 3\text{H}_2\text{O}$, and (d) $[\text{La}(\text{L})(\text{H}_2\text{O})\text{Cl}]\text{Cl}_2 \cdot 4\text{H}_2\text{O}$

residues were found after decomposition of the ligand. From DTA curve, it showed endothermic peaks with $t_{\text{max}} = 162^\circ\text{C}$ and 289°C , in which the lower temperature is closed to the melting point of the ligand. The overall weight loss amounted to 99.40% (calc. = 100%).

$[\text{UO}_2(\text{L})] \cdot 2\text{NO}_3$ complex showed two decomposition stages. The first stage is two steps. This stage was in the temperature range of 25–320°C, which congruent to the loss of 2HNO_3 and $\text{C}_{28}\text{H}_{25}\text{N}_7\text{S}$ molecules (found = 62.02% and calc. = 62.07%). The maximum temperature peaks were at 207°C and 294°C . This stage was accompanied by two endothermic peaks with $t_{\text{max}} = 138$ and 286°C on DTA curve. The second stage is

TABLE 1 Thermoanalytical results (TG, DTG, and DTA) of Schiff base (L) and its metal complexes

Compound	TG range (°C)	DTG _{max} (°C)	DTA _{max} (°C)	n	Mass loss total mass loss Estim (Calc.) %	Assignment	Residues
Schiff base (L)	170–530	262	162, 289	1	99.4 (100)	Loss of C ₃₃ H ₂₈ N ₈ S ₂	—
[UO ₂ (L)]—2NO ₃	25–320	207, 294	138, 286	2	62.02, (62.07)	Loss of 2HNO ₃ and C ₂₈ H ₂₅ N ₇ S	UO ₂
	320–645	431	406	1	10.57 (10.97), 72.59 (73.04)	Loss of C ₅ H ₃ NS	
[Er(L)(H ₂ O)Cl]Cl ₂ —3H ₂ O	40–160	77, 116	84	2	18.66 (18.35)	Loss of 2H ₂ O, Cl ₂ , HCl and C ₂ H ₆	½ Er ₂ O ₃
	160–900	217, 267	162	2	61.09 (61.43), 79.75 (79.78)	Loss of C ₃₁ H ₂₅ N ₈ S ₂ O _{0.5}	
[La(L)(H ₂ O)Cl]Cl ₂ —4H ₂ O	30–190	79, 159	81, 158	2	15.22 (15.23)	Loss of 3H ₂ O, HCl and C ₄ H ₄	½ La ₂ O ₃ + 5C
	190–525	228, 277	266, 417	2	61.14 (61.04), 76.36 (76.27)	Loss of Cl ₂ , C ₂₄ H ₂₈ N ₈ S ₂ O _{0.5}	

Note: n = number of decomposition steps.

one step. It was in the temperature range of 320–645°C represented the loss of C₅H₃NS molecule which accompanied by endothermic peak at $t_{max} = 406$ on DTA curve (found = 10.57% and calc. = 10.97%). The maximum temperature peak was at 431°C. Finally, the UO₂ oxide remained as residues with overall weight loss amounted to 72.59% (calc. = 73.04%).

[Er(L)(H₂O)Cl]Cl₂—3H₂O complex showed also two decomposition stages. The first stage is two steps in the temperature range of 40–160°C. Which congruent to the loss of two water molecules, Cl₂ gas, HCl, and C₂H₆ molecules (found = 18.66% and calc. = 18.35%). The maximum temperature peaks were at 77°C and 116°C. The second stage was also two steps. It was in the temperature range of 160–900°C represented the loss of C₃₁H₂₅N₈S₂O_{0.5} molecule (found = 61.09% and calc. = 61.43%), with maximum temperature peaks at 217°C and 267°C. The spectrum of DTA curve accompanied by two endothermic peaks at $t_{max} = 84$ °C and 162°C. Finally, the erbium oxide remained as residues with overall weight loss amounted to 79.75% (calc. = 79.78%).

[La(L)(H₂O)Cl]Cl₂—4H₂O complex showed also two decomposition stages. The first stage is two steps in the temperature range of 30–190°C, which congruent to the loss of three water molecules, HCl and C₄H₄ molecules (found = 15.22% and calc. = 15.23%). The maximum temperature peaks were at 79°C and 159°C. The second stage was also two steps. It was in the temperature range of 190–525°C represented the loss of Cl₂ gas and C₂₄H₂₈N₈S₂O_{0.5} molecules (found = 61.14% and calc. = 61.04%), with maximum temperature peaks at 228°C and 277°C. The spectrum of DTA curve accompanied by four endothermic peaks at $t_{max} = 81$ °C, 158°C, 266°C, and 417°C. Finally, the lanthanum oxide contaminated with carbon remained as residues with overall weight loss amounted to 76.36% (calc. = 76.27%).

3.1.9 | Antimicrobial activities

In vitro antibacterial activities of the Schiff base ligand, uranyl, erbium, and lanthanum complexes are given in Table 2. The solvent DMF is used as negative control, while Ampicillin is used as positive standard for antibacterial. Finally, the experiment is repeated three times under similar conditions.

The antibacterial activity of the prepared compounds investigated that the complexes showed higher activity than the ligand that had 0.0 mm/mg values. The order of their activity was represented as [UO₂(L)]—2NO₃ > [La(L)(H₂O)Cl]Cl₂—4H₂O < [Er(L)(H₂O)Cl]Cl₂—3H₂O > Ligand (L) against different four bacterial species.

The data showed that the activity values against *Bacillus subtilis* was 12, 12, and 11 mm/mg; *Staphylococcus aureus* was 15, 13, and 12 mm/mg; *Escherichia coli* was 13, 12, and 11 mm/mg; and *Pseudomonas aeruginosa* was 15, 13, and 13 mm/mg, for uranyl, lanthanum, and erbium complexes, respectively.

The difference in the effectiveness of the various compounds that prepared against any organisms depends up on the difference in the ribosome of the microbial cells or on their impermeability of the microbial cells.^[49] The metal complexes showed higher antimicrobial activity than the free Schiff base ligand. This increase may be as reason of the effect of metal ion on normal cell process. This phenomenon can be explained on the basis of Overton's concept.^[50] and chelation theory.^[51]

3.1.10 | Anticancer activities

The effect of ligand, uranyl, erbium, and lanthanum complexes on the growth of tumor cells was investigated

TABLE 2 Antibacterial activity of Schiff base (L) and its metal complexes

Sample	Inhibition zone diameter (mm/mg sample)			
	(Gram positive)		(Gram negative)	
	<i>Bacillus subtilis</i>	<i>Staphylococcus aureus</i>	<i>Escherichia coli</i>	<i>Pseudomonas aeruginosa</i>
Control: DMSO	0	0	0	0
Schiff base (L)	NA	NA	NA	NA
[UO ₂ (L)]—2NO ₃	12	15	13	15
[Er(L)(H ₂ O)Cl]Cl ₂ —3H ₂ O	11	12	11	13
[La(L)(H ₂ O)Cl]Cl ₂ —4H ₂ O	12	13	12	13
Ampicilin	26	21	25	26

Abbreviation: NA, no activity.

TABLE 3 Anticancer activities of Schiff base (L) and its metal complexes against MCF-7 and HepG2 cell lines

Compounds Conc. (μM)	Schiff base (L)	[UO ₂ (L)]—2NO ₃	[Er(L)(H ₂ O)Cl]—Cl ₂ —3H ₂ O	[La(L)(H ₂ O)Cl]—Cl ₂ —4H ₂ O
Surviving fraction (MCF-7)				
0.000	1.000	1.000	1.000	1.000
5.000	0.870	0.696	0.623	0.896
12.500	0.565	0.565	0.580	0.709
25.000	0.478	0.536	0.565	0.560
50.000	0.464	0.502	0.377	0.410
IC ₅₀	23	~50	35	36
Surviving fraction (HepG2)				
0.000	1.000	1.000	1.000	1.000
5.000	0.916	0.681	0.681	0.846
12.500	0.870	0.522	0.536	0.769
25.000	0.551	0.464	0.435	0.538
50.000	0.501	0.319	0.333	0.423
IC ₅₀	~50	17.6	18	33

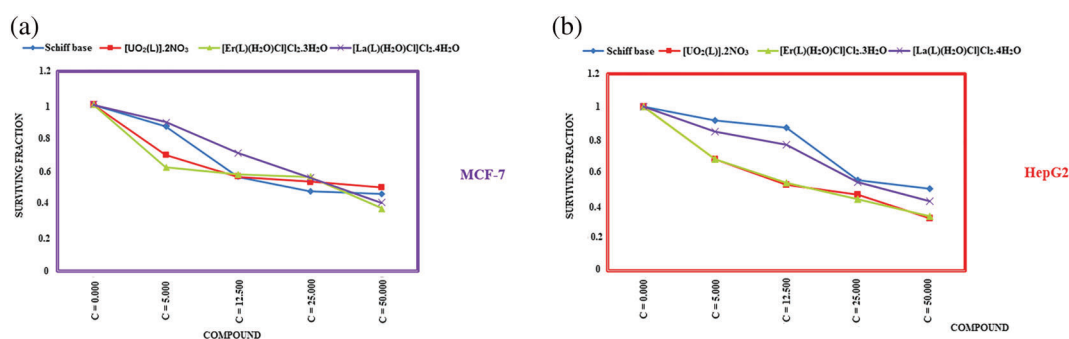


FIGURE 4 Anticancer activities of Schiff base ligand (L) and its metal complexes against (a) MCF-7 and (b) HepG2 cell lines

against two-cell line, as shown in Table 3. The synthesized compounds were recorded for their cytotoxic (Figure 4) effects against MCF-7 and HepG2 cell lines. Cultures were exposed to the prepared compounds at four different concentrations of (5, 12.5, 25, and 50 μM), and then, their IC₅₀ values were calculated. First, against

breast cancer cell line, the results appeared to be very good for the prepared compounds, at which the ligand showed the highest IC₅₀ value with 23 μM, while uranyl, erbium, and lanthanum complexes had ~50, 35, and 36 μM, respectively. Second, against hepatic cancer cell line, the prepared compounds showed results as

$[\text{UO}_2(\text{L})] \cdot 2\text{NO}_3$ (17.6 μM) > $[\text{Er}(\text{L})(\text{H}_2\text{O})\text{Cl}]\text{Cl}_2 \cdot 3\text{H}_2\text{O}$ (18 μM) > $[\text{La}(\text{L})(\text{H}_2\text{O})\text{Cl}]\text{Cl}_2 \cdot 4\text{H}_2\text{O}$ (33 μM) > Schiff base ligand (~ 50 μM). Their results indicated that the prepared compounds had good activities against different cell lines. From all the previous data, the ligand and its complexes showed anti-tumor activity that may be help in the future in-vivo researches and can be used after testing on different organisms as effective drugs for treatment of breast and hepatic carcinoma. The effective results of the metal complexes against different bacterial species and various anticancer cell lines may be due to the effect of the metal ion on the normal cell process according to Tweedy's chelation theory. Upon chelation, the polarity of the metal ions was decreased due to partial sharing of its positive charge with the possible π -electron delocalization and donor group in the whole complex

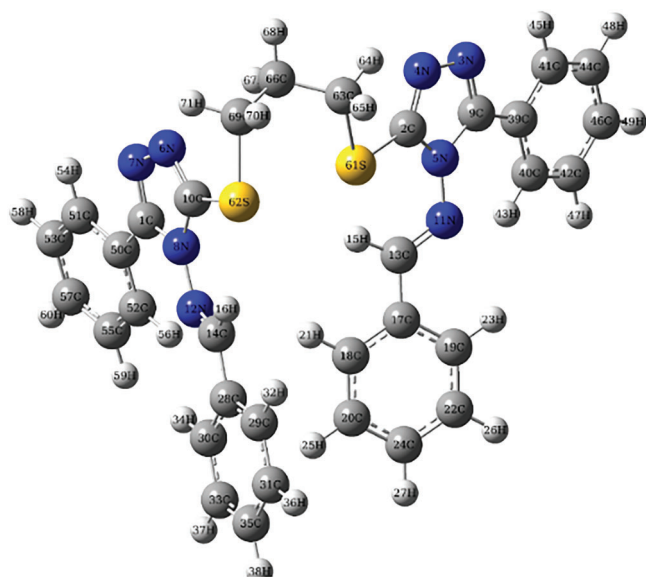


FIGURE 5 The optimized structure of triazole Schiff base ligand (L)

ring. Then, the lipophilic character of the central metal atom improved which increase the liposolubility and hydrophobic character of the complex. This cause the permeation through the lipid layers of the cell membrane of different organisms very easy.^[52]

3.2 | Theoretical characterization of the Schiff base ligand (L)

To confirm the successful preparation of the ligand, it was computed theoretically by DFT method. The optimized structure, some quantum parameters, MEP, and IR spectrum were reported. All data were compatible with the experimental one which confirming the preparation.

3.2.1 | Geometrical optimization of the ligand

The stable configuration of the triazole ligand was shown in Figure 5. The spheres had color as blue, yellow, and gray corresponding to N, S, and C atoms, respectively.^[20] Also, its bond length and angles were calculated and listed in Table S4. The dipole moment of the ligand was calculated from Gaussian 09, and its value is 8.6228 Debye. Furthermore, the total energy of the ligand appeared to be -2495.276 a.u.

3.2.2 | Molecular electrostatic potential

The electrostatic potential maps were calculated from DFT method for identification of the electronic charge distribution around molecular surface and then predicting the sites of reactions. The map of the ligand

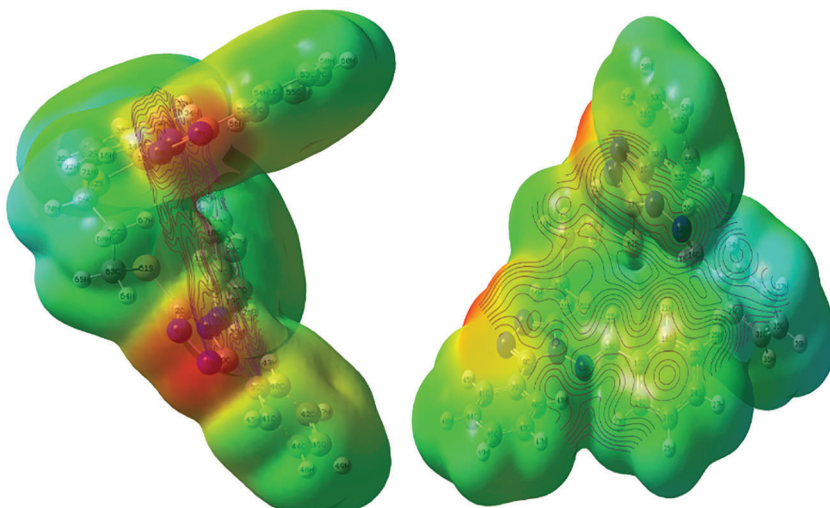


FIGURE 6 Molecular electrostatic potential map of Schiff base ligand (L), the electron density isosurface is 0.004 a.u.

was represented by using the same basis set of optimization.^[53] This 3D plot of molecular electrostatic potential (MEP) was showed in the Figure 6.

The map had different colors that corresponding to electron rich or poor area. The red color represents the electron-rich region (electrophilic attack), while blue color represents the electron-poor region (nucleophilic attack). The green color points to neutral electrostatic potential region.^[54] The ligand showed uniform distribution of charge density. The nitrogen and sulfur atoms were surrounded by a greater negative charge surface, making these sites potentially more favorable for electrophilic attack (red to orange). The aromatic rings appeared as green color.

3.2.3 | Mulliken charge analyses

The Mulliken electronegativity (Figure 7 and Table 4) also indicated the increase of electronegativity of sulfur and nitrogen atoms than the carbon atoms as represented from the results. These data indicated the favorable sites of donation (electrophilic attack) and the high probability of electron transfer from these atoms to the uranyl, erbium, and lanthanum ions in the proposed complexes^[55], where the nitrogen and sulfur atoms had more negative charges than the other atoms. The C1, C2, C9, and C10 atoms had higher positive atomic charges than the other carbon atoms. This was due to the attachment of sulfur and nitrogen atoms (electronegative atoms) to carbon atoms.

3.2.4 | Vibrational properties

Figure 8 showed theoretical IR spectrum of the ligand. Then, compare between the experimental and

calculated infrared spectra in the range of 4,000 to 400 cm^{-1} . The theoretical results had been calculated by using B3LYP/DFT. The vibrational frequencies computed by quantum chemical methods such as DFT reported some systematic errors. For overcoming

TABLE 4 The different Mulliken charges of Schiff base ligand

Atoms	Mulliken charges	Atoms	Mulliken charges
C1	0.632795	C30	0.040488
C2	0.19538	C31	0.023364
N3	-0.37799	C33	0.014136
N4	-0.3788	C25	0.025642
N5	-0.61736	C39	-0.05104
N6	-0.36785	C40	0.011845
N7	-0.37637	C41	0.0535
N8	-0.61731	C42	0.001446
C9	0.638785	C44	0.005753
C10	0.214411	C46	0.004388
N11	-0.31527	C50	-0.04915
N12	-0.3206	C51	0.058541
C13	0.390687	C52	0.009994
C14	0.388241	C53	0.01043
C17	-0.05096	C55	0.001834
C18	0.005402	C57	0.009877
C19	0.043974	S61	-0.41558
C20	0.016381	S62	-0.3959
C22	0.014631	C63	-0.09825
C24	0.014513	C66	0.103765
C28	-0.04547	C69	-0.09303
C29	0.017759		

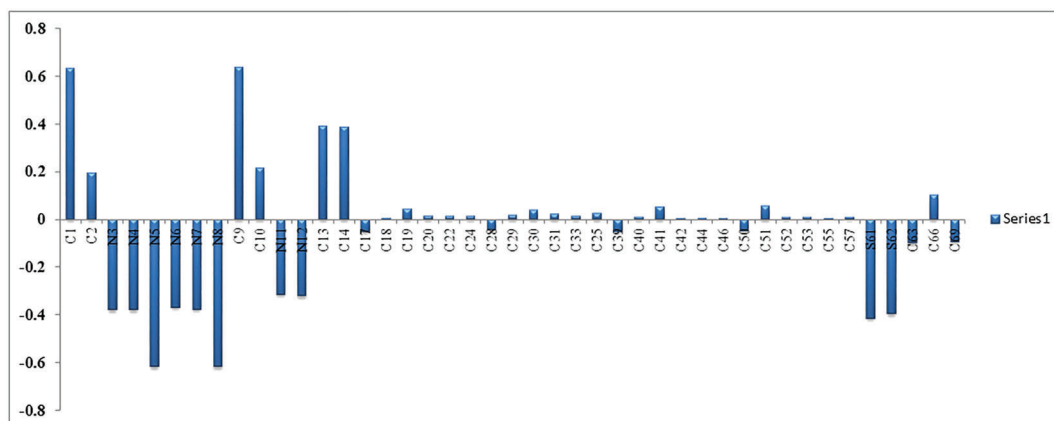
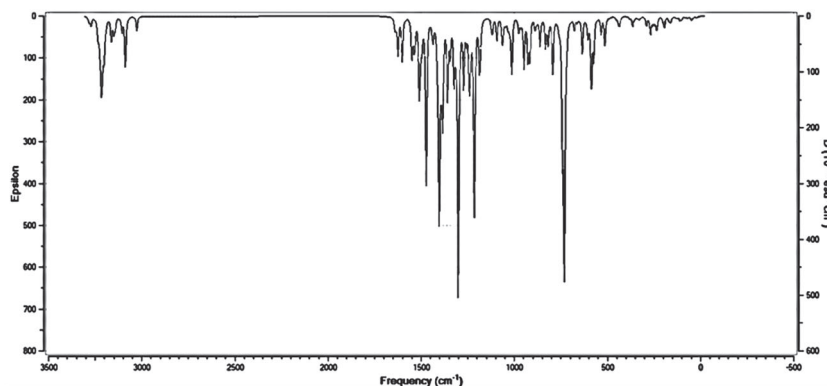


FIGURE 7 Mulliken charges of Schiff base ligand

FIGURE 8 Theoretical IR spectrum of the ligand

TABLE 5 Energy values obtained in docking calculations of ligand (L), [UO₂(L)]·2NO₃, [Er(L)(H₂O)Cl]Cl₂·3H₂O, and [La(L)(H₂O)Cl]Cl₂·4H₂O with 3HB5 and 2GYT receptors

Compound	Receptor	Ligand moiety	Receptor site	Interaction	Distance (Å)	E (kcal/mol)
Ligand (L)	3HB5	N7	N, GLY, 92, (X)	H—acceptor	3.35	−0.9
		N11	NZ, LYS, 195, (X)	H—acceptor	3.42	−1.9
		6-ring	NE, ARG, 37, (X)	π—cation	3.87	−0.7
		5-ring	NZ, LYS, 195, (X)	π—cation	4.69	−6.8
	2GYT	S61	OXT, LYS, 76, (A)	H—donor	3.94	−1.7
		S62	O, LYS, 76, (A)	H—donor	3.80	−0.4
		S62	OXT, LYS, 76, (A)	H—donor	3.80	−0.3
		6-ring	NZ, LYS, 4, (A)	π—cation	3.82	−1.2
		5-ring	CG, GLN, 13, (A),	π—H	4.30	−0.9
		6-ring	CB, MET, 75, (A),	π—H	4.20	−0.7
[UO ₂ (L)]·2NO ₃ complex	3HB5	N7	N, GLY, 92, (X)	H—acceptor	3.16	−2.9
		6-ring	NE, ARG, 37, (X)	π—cation	3.85	−1.3
		6-ring	NH2, ARG, 37, (X)	π—cation	3.60	−0.6
		6-ring	CB, ALA, 91, (X)	π—H	4.20	−0.8
		6-ring	NZ, LYS, 195, (X)	π—cation	4.46	−3.9
	2GYT	O73	NZ, LYS, 4, (A)	H—acceptor	2.63	−28.0
		O74	NZ, LYS, 4, (A)	H—acceptor	2.85	−2.2
[Er(L)(H ₂ O)Cl]Cl ₂ ·3H ₂ O complex	3HB5	S61	O, GLY, 92, (X)	H—donor	3.37	−4.1
		S62	O, GLY, 9, (X)	H—donor	4.03	−1.3
		O74	O, GLY, 92, (X)	H—donor	2.73	−4.6
		N6	N, SER, 11, (X)	H—acceptor	3.04	−3.9
		Er72	NH2, ARG, 37, (X)	ionic	2.92	−5.0
	2GYT	N7	NZ, LYS, 4, (A)	H—acceptor	3.29	−3.8
	[La(L)(H ₂ O)Cl]Cl ₂ ·4H ₂ O complex	3HB5	N3	NZ, LYS, 40, (X)	H—acceptor	3.34
2GYT		N4	SD, MET, 1, (A),	H—donor	3.95	−0.3
		Cl72	O, LYS, 76, (A),	H—donor	3.47	−2.5

these systematic errors, it used a scaling factor as 0.9648 for LanL2DZ (which can be formed from harmonicity).^[56]

The experimental bands of the ligand were observed at 1,603, 1,571, and 767 cm^{-1} that corresponded to azomethine, triazole moiety, and C—S vibrations, respectively, and theoretically, these bands are computed at 1625.17, 1,551.32, and 793.73 cm^{-1} , respectively.^[57] The results confirmed the successful preparation of the triazole ligand.

3.2.5 | Molecular modeling of Schiff base ligand (L), $[\text{UO}_2(\text{L})]-2\text{NO}_3$, $[\text{Er}(\text{L})(\text{H}_2\text{O})\text{Cl}]\text{Cl}_2-3\text{H}_2\text{O}$ and $[\text{La}(\text{L})(\text{H}_2\text{O})\text{Cl}]\text{Cl}_2-4\text{H}_2\text{O}$ complexes with different receptors: Docking study

The ligand, uranyl (II), erbium (III), and lanthanum (III) complexes were subjected to molecular docking with 3HB5 and 2GYT receptors using Auto Dock Tools. This is theoretical tool that used to confirm the results observed

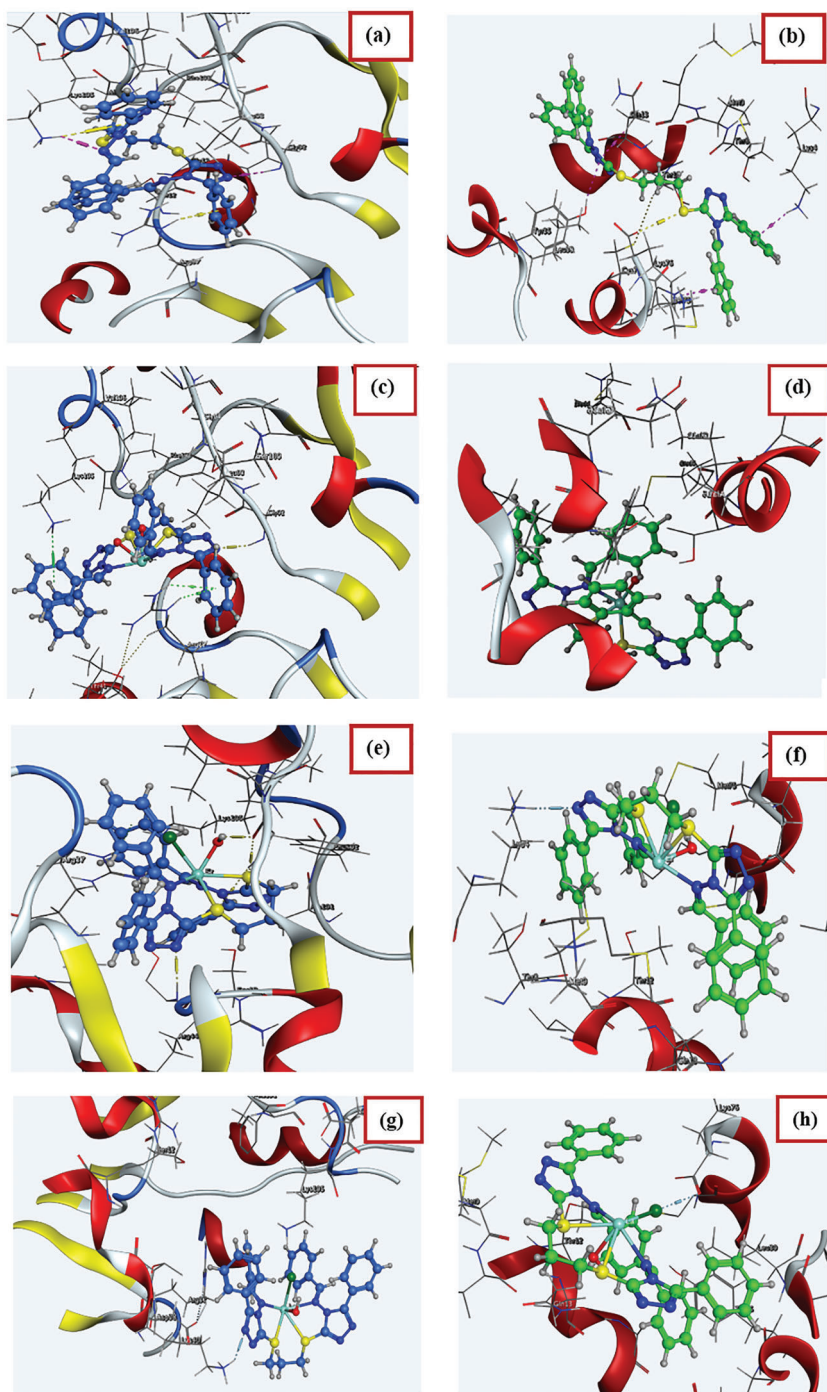


FIGURE 9 Three-dimensional plots of the interaction between Schiff base with receptors of (a) 3HB5, (b) 2GYT, $[\text{UO}_2(\text{L})]-2\text{NO}_3$ with receptors of (c) 3HB5, (d) 2GYT, $[\text{Er}(\text{L})(\text{H}_2\text{O})\text{Cl}]\text{Cl}_2-3\text{H}_2\text{O}$ with receptors of (e) 3HB5 and (f) 2GYT, and $[\text{La}(\text{L})(\text{H}_2\text{O})\text{Cl}]\text{Cl}_2-4\text{H}_2\text{O}$ with receptors of (g) 3HB5 and (h) 2GYT

from experimental anticancer activities. They were analyzed for their docking conformations in terms of binding energy, hydrogen bonding, and hydrophobic interactions with different protein receptors.^[57,58] The crystal structure of these receptors was obtained from the protein data bank. Finally, the results of different types of bonding and minimum energy values were listed in Table 5. The 3D plots of the interaction of the prepared compounds with different receptors were also represented in Figure 9.

First, the compounds were investigated against crystal structure of breast cancer mutant oxidoreductase (PDB ID: 3HB5). The ligand showed four interactions with amino acids LYS, ARG, and GLY. These interactions were H—acceptors and pi—cation bonds, in which the ligand showed the lowest binding energy -6.8 kcal/mol, while uranyl, erbium, and lanthanum complexes showed some different interaction besides H—acceptors and pi—cation as H—donor, pi—H, and ionic bonds. The binding energies were appeared at -3.9 , -4.1 , and -5.0 for $[\text{UO}_2(\text{L})]-2\text{NO}_3$ (~ 50 μM), $[\text{La}(\text{L})(\text{H}_2\text{O})\text{Cl}]\text{Cl}_2-4\text{H}_2\text{O}$ (36 μM), and $[\text{Er}(\text{L})(\text{H}_2\text{O})\text{Cl}]\text{Cl}_2-3\text{H}_2\text{O}$ (35 μM) complexes, respectively. The data confirmed the results reported previously about MCF-7 cell line of anticancer activity as $\text{L} > \text{Er-L} > \text{La-L} > \text{UO}_2\text{-L}$.

Second, the compounds were investigated against crystal structure of hepatic cancer (PDB ID: 2GYT). The ligand reported six interactions with various amino acids as LYS, GLN, and MET. These interactions were H—donor, pi—cation, and pi—H bonds, with binding energy value -1.7 kcal/mol. H-acceptor interaction was appeared in Er—L, H—donor interaction for La—L, and H—acceptor and ionic bonds for $\text{UO}_2\text{-L}$. The values of their binding energies were -28.0 , -3.8 , and -2.5 kcal/mol for $[\text{UO}_2(\text{L})]-2\text{NO}_3$ (17.6 μM), $[\text{Er}(\text{L})(\text{H}_2\text{O})\text{Cl}]\text{Cl}_2-3\text{H}_2\text{O}$ (18 μM), and $[\text{La}(\text{L})(\text{H}_2\text{O})\text{Cl}]\text{Cl}_2-4\text{H}_2\text{O}$ (33 μM), respectively. Furthermore, these data confirmed the results reported previously about HepG2 cell line of anticancer activity as $\text{UO}_2\text{-L} > \text{Er-L} > \text{La-L} > \text{L}$.

Finally, these theoretical data from molecular docking well confirmed the experimental results that appeared about anticancer activity of the ligand and its complexes.

3.2.6 | Structural interpretation

The structures of uranyl (II), erbium (III), and lanthanum (III) complexes were elucidated by elemental analysis, IR, $^1\text{H-NMR}$, MS, molar conductance, UV/Vis, and thermal analyses. Then, their structures were represented in Figure 10.

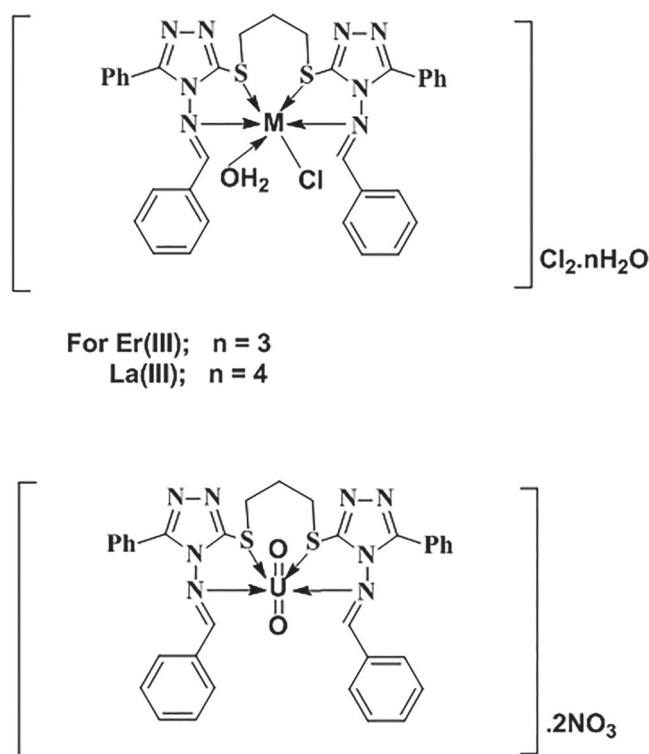


FIGURE 10 Structure of $[\text{UO}_2(\text{L})]-2\text{NO}_3$, $[\text{Er}(\text{L})(\text{H}_2\text{O})\text{Cl}]\text{Cl}_2-3\text{H}_2\text{O}$, and $[\text{La}(\text{L})(\text{H}_2\text{O})\text{Cl}]\text{Cl}_2-4\text{H}_2\text{O}$ complexes

4 | CONCLUSION

The present investigation described the synthesis, experimental, and theoretical characterization of bis (amino triazole) Schiff base ligand by using DFT method. Its uranyl (II), erbium (III), and lanthanum (III) complexes were also prepared. The compounds were investigated against four bacteria species. Also, their anticancer activities against two cell lines (MCF-7 and HepG2) were screened. From elemental analysis data, it was shown that the ligand was prepared in 1:2 ratio of 1,3-bis(4-amino-5-phenyl-1,2,4-triazol-3-ylsulfanyl)propane with benzaldehyde, while the complexes were prepared in 1:1 molar ratio with metal ions. IR spectral data reported that ligand behaved as a neutral tetradentate N,N,S,S-ligand. Conductivity measurements indicated that the $\text{UO}_2(\text{II})$, Er (III), and La (III) complexes are 1:2 electrolytes. All complexes had octahedral geometry. Their bacterial activity against two Gram-positive bacteria (*Bacillus subtilis* and *Staphylococcus aureus*) and two Gram-negative bacteria (*Escherichia coli* and *Pseudomonas aeruginosa*) showed that ligand had no activity against four types of bacteria but $\text{UO}_2(\text{II})$ had the higher bacterial activity. The anticancer activity indicated that ligand had the lowest IC_{50} value (23 μM) for MCF-7 cell line, while the $[\text{UO}_2(\text{L})]-2\text{NO}_3$ complex had

the lowest IC₅₀ value (17.6 μM) for HepG2 cell line. The study of molecular docking between the three prepared compounds with receptors of 3HB5 and 2GYT was investigated for confirming the experimental anticancer activity results.

AUTHOR CONTRIBUTIONS

Reem Deghadi: Formal analysis; methodology; resources. **Ashraf Abbas:** Data curation; formal analysis; methodology; resources. **Gehad Mohamed:** Data curation; project administration; supervision.

DATA AVAILABILITY STATEMENT

The data that support the findings of this study are available on request from the corresponding author. The data are not publicly available due to privacy or ethical restrictions.

ORCID

Reem G. Deghadi  <https://orcid.org/0000-0002-4988-8907>

Ashraf A. Abbas  <https://orcid.org/0000-0001-7061-9907>

Gehad G. Mohamed  <https://orcid.org/0000-0002-1525-5271>

REFERENCES

- [1] H. Q. Chang, L. Jia, J. Xu, T. F. Zhu, Z. Q. Xu, R. H. Chen, T. L. Ma, Y. Wang, W. N. Wu, *J. Mol. Struct.* **2015**, *1106*, 366.
- [2] K. J. Davis, C. Richardson, J. L. Beck, B. M. Knowles, A. Guedin, J. L. Mergny, A. C. Willis, S. F. Ralph, *Dalton Trans.* **2015**, *44*, 3136.
- [3] S. Khani, M. Montazerzohori, R. Naghiha, *J. Phys. Org. Chem.* **2018**, *31*(12), e3873.
- [4] H. Makio, N. Kashiwa, T. Fujita, *Adv. Syn. Catalysis.* **2002**, *344*(5), 477.
- [5] T. D. Pasatou, J. P. Sutter, A. M. Madalan, F. Z. Fellah, C. Duhayon, M. Andruh, *Inorg. Chem.* **2011**, *50*(13), 5890.
- [6] S. A. Mousavi, M. Montazerzohori, R. Naghiha, A. Masoudias, S. Mojahedi, T. Doert, *Appl. Organomet. Chem.* **2020**, *34*(4), e5550.
- [7] L. Mishra, S. K. Dubey, *Spectrochim. Acta. Part A* **2007**, *68*, 364.
- [8] P. M. Ronad, M. N. Noolvi, S. Sapkal, S. Dharbhamulla, V. S. Maddi, *Eur. J. Med. Chem.* **2010**, *45*, 85.
- [9] G. Ceyhan, M. Tümer, M. Kose, V. McKee, S. Akar, *JOL* **2012**, *132*, 2917.
- [10] W. A. Abbas, A. S. Al-Hamdani, I. P. Widiyantara, R. G. Hamoodah, Y. G. Ko, *J. Phys. Org. Chem.* **2017**, *30*(12), e3707.
- [11] L. Touafri, A. Hellal, S. Chafaa, A. Khelifa, A. Kadri, *J. Mol. Struct.* **2017**, *1149*, 750.
- [12] M. Montazerzohori, S. M. Jahromi, A. Naghiha, *J. Indust. Eng. Chem.* **2014**, *22*, 248.
- [13] U. Yunus, M. H. Bhatti, N. Rahman, N. Mussarat, S. Asghar, B. Masood, *J. Chem.* **2013**, 8.
- [14] N. G. Kandile, M. I. Mohamed, H. M. Ismaeel, *J. Enzyme Inhib. Med. Chem.* **2017**, *32*(1), 119.
- [15] K. M. Khan, S. Siddiqui, M. Saleem, M. Taha, S. M. Saad, S. Perveen, M. I. Choudhary, *Bioorg. Med. Chem.* **2014**, *22*, 6509.
- [16] K. El Akri, K. Bougrin, J. Balzarini, A. Faraj, R. Benhida, *Bioorg. Med. Chem. Lett.* **2007**, *17*(23), 6656.
- [17] A. F. Alghamdi, N. Rezki, *J. Taibah Univer. Sci.* **2017**, *11* (5), 759.
- [18] P. Tyagi, M. Tyagi, S. Agrawal, S. Chandra, H. Ojha, M. Pathak, *Spectrochim. Acta A* **2017**, *171*, 246.
- [19] J. L. Sonnenberg, P. J. Hay, R. L. Martin, B. E. Bursten, *Inorg. Chem.* **2005**, *44*, 2255.
- [20] X. L. Li, J. Luo, Y. W. Lin, L. F. Liao, C. M. Nie, *J. Radioanal. Nucl. Chem.* **2016**, *307*, 407.
- [21] X. Shen, L. Liao, L. Chen, Y. He, C. Xu, X. Xiao, Y. Lin, C. Nie, *Spectrochim. Acta A* **2014**, *123*, 110.
- [22] A. L. El-Ansary, N. S. Abdel-Kader, *Inter. J. Inorg. Chem.* **2012**, 13 pages
- [23] A. H. M. Elwahy, A. A. Abbas, Y. A. Ibrahim, *J. Chem. Res.* **1996**, *4*, 182.
- [24] A. Albert, *Selective Toxicity: Physico-Chemical Basis of Therapy*, 6th ed., Wiley, New York **1979**.
- [25] S. Chandra, D. Jain, A. K. Sharma, P. Sharma, *Molecules* **2009**, *14*(1), 174.
- [26] P. Skehan, R. Storeng, D. Scudiero, A. Monks, J. McMahon, D. Vistica, J. T. Warren, H. Bokesch, S. Kenney, M. R. Boyd, *J. National Cancer Instit.* **1990**, *82*(13), 1107.
- [27] C. J. Dhanaraj, I. U. Hassan, J. Johnson, J. Joseph, R. S. Joseyphus, *J. Photochem. Photobiol. B* **2016**, *162*, 115.
- [28] C. Balakrishnan, L. Subha, M. A. Neelakantan, S. S. Mariappan, *Spectrochim. Acta A* **2015**, *150*, 671.
- [29] M. J. Frisch, *Gaussian 03, Revision C.01*, Gaussian Inc, Wallingford CT **2004**.
- [30] G. G. Mohamed, Z. H. Abd El-Wahab, *Spectrochim. Acta A* **2005**, *61*, 1059.
- [31] R. Dennington, T. Keith, J. Millam, editors *GaussView, Version 5.0.8*, R.K.S, Semichem Inc., Shawnee Mission, Dennington **2009**.
- [32] W. H. Mahmoud, R. G. Deghadi, G. G. Mohamed, *Arabian J. Chem.* **2020**, *13*, 5390.
- [33] G. G. Mohamed, E. M. Zayed, A. M. M. Hindy, *Spectrochim. Acta A* **2015**, *145*, 76.
- [34] A. S. Munde, A. N. Jagdale, S. M. Jadhav, T. K. Chondhekar, *J. Serb. Chem. Soc.* **2010**, *75*(3), 349.
- [35] A. Antony, F. Fasna, P. A. Ajil, J. T. Varkey, *Res. Rev. J. Chem.* **2016**, *5*(2), 37.
- [36] M. Shakir, M. Azam, M. F. Ullah, S. M. Hadi, *J. Photochem. Photobiol. B* **2011**, *104*, 449.
- [37] M. Gabera, H. A. El-Ghamry, S. K. Fathalla, M. A. Mansour, *Mater. Sci. Eng. C* **2018**, *83*, 78.
- [38] R. C. Maurya, B. Shukla, J. Chourasia, S. Roy, P. Bohre, S. Sahu, M. H. Martin, *Arabian J Chem* **2015**, *8*(5), 655.
- [39] L. J. Bellamy, *The IR spectra of complex molecules*, Ethuen, London **1985**.
- [40] H. A. ElGhamry, R. G. El-Sharkawy, M. Gaber, *J. Iran. Chem. Soc.* **2014**, *11*, 379.
- [41] A. Rauf, A. Shah, K. S. Munawar, A. A. Khan, R. Abbasi, M. A. Yameen, A. M. Khan, A. R. Khan, I. Z. Qureshi, H. B. Kraatz, Z. Rehman, *J. Mol. Struct.* **2017**, *1145*, 132.
- [42] R. G. Deghadi, W. H. Mahmoud, G. G. Mohamed, *Appl. Organomet. Chem.* **2020**, *34*(10), e5883.

- [43] S. Muche, I. Levacheva, O. Samsonova, A. Biernasiuk, A. Malm, R. Lonsdale, L. Popiołek, U. Bakowsky, M. Holyńska, *J. Mol. Struct.* **2017**, *1127*, 231.
- [44] D. Xu, Q. Sun, Z. Quan, W. Sun, X. Wang, *Tetrahedron: Asymmetry* **2017**, *28*, 954.
- [45] M. A. Arafath, F. Adam, M. R. Razali, L. E. A. Hassan, M. B. K. Ahamed, A. M. S. A. Majd, *J. Mol. Struct.* **2017**, *1130*, 791.
- [46] M. Barwiolek, J. Sawicka, M. Babinska, A. Wojtczak, A. Surdykowski, R. Szczesny, E. Szlyk, *Polyhedron* **2017**, *135*, 153.
- [47] A. A. Abdel Aziz, S. H. Seda, *Appl. Organomet. Chem.* **2017**, *31*(12), e3879.
- [48] M. A. Neelakantan, S. S. Marriappan, J. Dharmaraja, T. Jeyakumar, K. Muthukumaran, *Spectrochim. Acta A* **2008**, *71*, 628.
- [49] J. D. Chellaian, J. Johnson, *Spectrochim. Acta A* **2014**, *127*, 396.
- [50] S. A. Sadeek, W. H. El-Shwiniy, W. A. Zordok, A. M. El-Didamony, *J. Argent. Chem. Soc.* **2009**, *97*, 128.
- [51] B. G. Tweedy, *Phytopathology* **1964**, *25*, 910.
- [52] R. Fekri, M. Salehi, A. Asadi, M. Kubicki, *J. Inorg. Chim. Acta.* **2019**, *484*, 245.
- [53] W. H. Mahmoud, G. G. Mohamed, O. Y. El-Sayed, *Appl. Organomet. Chem.* **2017**, *32*(2), e4051.
- [54] W. H. Mahmoud, R. G. Deghadi, G. G. Mohamed, *Appl. Organomet. Chem.* **2017**, *32*(4), 4289.
- [55] W. H. Mahmoud, N. F. Mahmoud, G. G. Mohamed, *Appl. Organomet. Chem.* **2017**, *31*(12), e3858.
- [56] H. Vural, M. Orbay, *J. Mol. Struct.* **2017**, *1146*, 669.
- [57] W. H. Mahmoud, R. G. Deghadi, G. G. Mohamed, *Indian J. Chem.* **2019**, *58A*, 1319.
- [58] W. H. Mahmoud, R. G. Deghadi, M. M. I. El Desssouky, *Appl. Organomet. Chem.* **2019**, *33*, e4556.

SUPPORTING INFORMATION

Additional supporting information may be found online in the Supporting Information section at the end of this article.

How to cite this article: R. G. Deghadi, A. A. Abbas, G. G. Mohamed, *Appl Organomet Chem* **2021**, e6292. <https://doi.org/10.1002/aoc.6292>